Electronic Research Archive

https://www.aimspress.com/journal/era

ERA, 32(11): 6424–6442.
DOI: 10.3934/era.2024299
Received: 26 August 2024
Revised: 31 October 2024
Accepted: 13 November 2024
Published: 25 November 2024

Research article

Dynamic behaviors of a Leslie-Gower predator-prey model with Smith growth and constant-yield harvesting

Mengxin He[1] **and Zhong Li**[2,*]

[1] School of Computer and Big Data, Minjiang University, Fuzhou, Fujian 350108, China
[2] School of Mathematics and Statistics, Fuzhou University, Fuzhou, Fujian 350108, China

* **Correspondence:** Email: lizhong04108@163.com.

Abstract: A Leslie-Gower predator-prey model with Smith growth and constant-yield harvesting is proposed in this paper. We show that the system admits at most two boundary equilibria, both of which are unstable. The degenerate positive equilibrium of the system is a cusp of codimension 2, and the system undergoes cusp-type Bogdanov-Takens bifurcation of codimension 2. Moreover, we prove that the system has a weak focus of order at most 3, and the system can undergo a degenerate Hopf bifurcation of codimension 3. Our results reveal that the constant-yield harvesting can lead to richer dynamic behaviors.

Keywords: Leslie-Gower; harvesting; Hopf bifurcation; Bogdanov-Takens bifurcation; Smith growth

1. Introduction

The traditional predator–prey model was built to explain the survival of marine fish, which has been extensively researched and improved to more accurately describe the development of populations. However, there is no upper limit to the growth rate of predators, which is not suitable for most populations in nature. Based on this fact, Leslie [1,2] considered that the growth rates of both predator and prey have upper limits by assuming that the "carrying capacity" of the predator's environment is proportional to the number of prey and proposed the following well-known Leslie–Gower model:

$$\begin{aligned} \dot{x} &= rx\Big(1-\frac{x}{K}\Big)-\beta xy,\\ \dot{y} &= \delta y\Big(1-\frac{y}{nx}\Big), \end{aligned} \tag{1.1}$$

where $\frac{y}{nx}$ denotes the Leslie–Gower term and nx is the "carrying capacity" of the predator. Korobeinikov [3] successively verified that the fixed point of the Leslie–Gower model is globally stable.

System (1.1) was modified by introducing different types of functional response, and the stability and bifurcations were analyzed [4–10].

In the above system, the average growth rate $\frac{\dot{x}}{x}$ of the traditional logistic model is a linear function of the prey. However, in 1963, Smith [11] found that the average growth rate of large daphnia populations does not follow linear functions and demonstrated that food is needed for the maintenance and growth of the population during the growth stage but is only required for maintenance when the population reaches saturation. Then proposed the "limited food" model, sometimes called the "limited resources" model. When introducing Smith growth into system (1.1), the system takes the following form:

$$\begin{aligned} \dot{x} &= rx\Big(\frac{K-x}{K+ax}\Big) - \beta xy, \\ \dot{y} &= \delta y\Big(1 - \frac{y}{nx}\Big), \end{aligned} \tag{1.2}$$

where $rx(\frac{K-x}{K+ax})$ is the Smith growth function. With the influence of environmental toxicants, Kumar [12] discussed the spatiotemporal dynamics and delay-induced instability of a Leslie-Gower prey-predator model with Smith growth rate. Li and He [13] studied the Hopf bifurcation of a delayed food-limited model with feedback control; Feng et al. [14] considered the stability and Hopf bifurcation of a modified Leslie-Gower predator–prey model with Smith growth rate and Beddington-DeAngelis functional response; Bai et al. [15] proposed a predator–prey model with a Smith growth function and the additive predation in prey and studied the stability and Hopf bifurcation of the system. For more results on dynamical behaviors of systems with Smith growth function, please see [16, 17].

On the other hand, sustainable harvesting plays an important role in maintaining ecological balance, and its influence on population development has been extensively studied. Huang et al. [18] investigated the bifurcation of predator-prey models with constant-yield prey harvesting. Xu et al. [19] discussed the degenerate Bogdanov-Takens bifurcation of a Holling-Tanner predator-prey model with constant-yield prey harvesting. Wu et al. [20] studied the bifurcations such as the degenerate Bogdanov-Takens bifurcation and degenerate Hopf bifurcation of a Holling-Tanner model with generalist predator and constant-yield prey harvesting. Zhu and Lan [21] modified system (1.1) by introducing constant-yield prey harvesting

$$\begin{aligned} \dot{x} &= rx\Big(1 - \frac{x}{K}\Big) - \beta xy - H, \\ \dot{y} &= \delta y\Big(1 - \frac{y}{nx}\Big), \end{aligned} \tag{1.3}$$

where $H > 0$ is the constant-yield prey harvesting. The authors discussed the saddle node bifurcation, supercritical, and subcritical Hopf bifurcations of the system.

Motivated by systems (1.2) and (1.3), in this paper we propose the following system:

$$\begin{aligned} \dot{x} &= rx\Big(\frac{K-x}{K+ax}\Big) - \beta xy - H, \\ \dot{y} &= \delta y\Big(1 - \frac{y}{nx}\Big), \end{aligned} \tag{1.4}$$

where $x(t)$ and $y(t)$ are the densities of the prey and predator at time t, respectively; $r > 0$ and $\delta > 0$ are the intrinsic growth rates of the prey and predator, respectively; $K > 0$ is the carrying capacity of

the prey; $\beta > 0$ is the maximum rate of predation; $H > 0$ is the constant-yield prey harvesting; $\frac{r}{a}$ with $a > 0$ is the mass substitution rate of the population at K; $n > 0$ is the quality of prey provided to the predator.

For simplicity, we make the following transformations:

$$\overline{x} = \frac{x}{K}, \quad \overline{y} = \frac{y}{nK}, \quad \overline{t} = rt,$$

and drop the bars, then system (1.4) can be rewritten as

$$\begin{aligned} \dot{x} &= \frac{x(1-x)}{1+ax} - bxy - h, \\ \dot{y} &= sy\Big(1 - \frac{y}{x}\Big), \end{aligned} \tag{1.5}$$

where

$$b = \frac{\beta nK}{r}, \qquad h = \frac{H}{rK}, \qquad s = \frac{\delta}{r}.$$

We can easily verify that all the solutions of system (1.5) are positive and bounded with positive initial conditions.

The rest of the paper is organized as follows: In Section 2, we will investigate the existence and stability of the boundary and positive equilibria of system (1.5). In Section 3, we will prove the Bogdanov–Takens bifurcation of codimension 2 and the degenerate Hopf bifurcation of codimension 3. In Section 4, we will present some bifurcation diagrams and phase portraits to support our theoretical results. We give a brief discussion in the last section.

2. Existence and stability of equilibria

In this section, we discuss types of the boundary and positive equilibria of system (1.5) in a positive invariant and bounded region

$$\Omega = \{(x, y) | 0 < x < 1,\ 0 \le y < 1\}.$$

For any nonnegative equilibrium $E(x, y)$, the Jacobian matrix of system (1.5) is

$$J_E = \begin{pmatrix} \dfrac{1-2x-ax^2}{(1+ax)^2} - by & -bx \\ \dfrac{sy^2}{x^2} & s\Big(1 - \dfrac{2y}{x}\Big) \end{pmatrix},$$

and

$$\begin{aligned} \mathrm{Det}(J_E) &= s\Big(\frac{1-2x-ax^2}{(1+ax)^2} - by\Big)\Big(1 - \frac{2y}{x}\Big) + \frac{sby^2}{x}, \\ \mathrm{Tr}(J_E) &= \frac{1-2x-ax^2}{(1+ax)^2} - by - \frac{2sy}{x} + s. \end{aligned}$$

2.1. Existence and stability of boundary equilibria

Substituting $y = 0$ into the first equation of (1.5), we have

$$f_0(x) = x^2 + (ah - 1)x + h,$$

whose discriminant is

$$\Delta_{f_0} = (1 - ah)^2 - 4h.$$

Denote

$$x_{10} = \frac{1 - ah - \sqrt{\Delta_{f_0}}}{2}, \quad x_{20} = \frac{1 - ah + \sqrt{\Delta_{f_0}}}{2} \quad \text{and} \quad \bar{x}_* = \frac{1 - ah}{2}.$$

Then we have the following theorem.

Theorem 2.1. *For the boundary equilibria of system* (1.5)*, we have:*

(1) *If* $h < \frac{1}{4}$ *and* $0 < a < \frac{1-2\sqrt{h}}{h}$*, then system* (1.5) *has two boundary equilibria: an unstable node* $E_{10}(x_{10}, 0)$ *and a saddle* $E_{20}(x_{20}, 0)$*;*

(2) *if* $h < \frac{1}{4}$ *and* $a = \frac{1-2\sqrt{h}}{h}$*, then system* (1.5) *has a unique boundary equilibrium* $\bar{E}_*(\bar{x}_*, 0)$*, which is a saddle node, including an unstable parabolic sector in the left.*

Proof. If $ah < 1$ and $\Delta_{f_0} > 0$, that is $h < \frac{1}{4}$ and $0 < a < \frac{1-2\sqrt{h}}{h}$, $f_0(x)$ has two positive roots in the interval $(0, 1)$, which implies that system (1.5) has two boundary equilibria $E_{10}(x_{10}, 0)$ and $E_{20}(x_{20}, 0)$.

If $ah < 1$ and $\Delta_{f_0} = 0$, that is $h < \frac{1}{4}$ and $a = \frac{1-2\sqrt{h}}{h}$, $f_0(x)$ has a unique positive root in the interval $(0, 1)$, which implies that system (1.5) has a unique boundary equilibrium $\bar{E}_*(\bar{x}_*, 0)$.

The Jacobian matrix of system (1.5) at $E_0(x, 0)$ is

$$J_{E_0} = \begin{pmatrix} \dfrac{1 - 2x - ax^2}{(1 + ax)^2} & -bx \\ 0 & s \end{pmatrix}.$$

We can easily verify that

$$(1 - 2x - ax^2)|_{x=x_{10}} > 0, \quad (1 - 2x - ax^2)|_{x=x_{20}} < 0, \quad (1 - 2x - ax^2)|_{x=\bar{x}_*} = 0.$$

Hence, E_{10} is an unstable node and E_{20} is a saddle.

When $a = \frac{1-2\sqrt{h}}{h}$, make the following transformations successively

$$\begin{aligned} x &= x_1 + \frac{1 - ah}{2}, \quad y = y_1; \\ x_1 &= x_2 - b\sqrt{h}y_2, \quad y_1 = sy_2, \end{aligned}$$

then system (1.5) becomes

$$\begin{aligned} \dot{x}_2 &= \frac{\sqrt{h}}{s(\sqrt{h} - 1)}x_2^2 - b\left(1 + \frac{2h}{s(\sqrt{h} - 1)}\right)x_2y_2 + b\left(b\sqrt{h} - s + \frac{bh\sqrt{h}}{(\sqrt{h} - 1)s}\right)y_2^2 + o(|x_2, y_2|^2), \\ \dot{y}_2 &= y_2 - \frac{s}{\sqrt{h}}y_2^2 + o(|x_2, y_2|^2). \end{aligned} \tag{2.1}$$

By Theorem 7.1 in Chapter 2 of Zhang et al. [22], $\bar{E}_*$ is a saddle node, which includes an unstable parabolic sector in the left if $h < \frac{1}{4}$ and $a = \frac{1-2\sqrt{h}}{h}$. The proof is completed.

Choose $(h, b, s) = (0.08, 1.2, 0.1)$, and we present the relationship between the boundary equilibria of system (1.5) and a, as well as the phase portrait when $a = 0.1$, shown in Figure 1. Figure 1(a) shows that when $0 < a < 5.428932188$, system (1.5) has two boundary equilibria; when $a \doteq 5.428932188$,

system (1.5) has a unique boundary equilibrium; and when $a > 5.428932188$, system (1.5) has no boundary equilibrium. Figure 1(b) shows that system (1.5) admits two boundary equilibria, where E_{10} is an unstable node and E_{20} is a saddle. Further, when the initial values lie inside the region to the right of the stable manifold of the saddle (the positive equilibrium), both populations will coexist in fixed sizes; otherwise, both populations will not coexist.

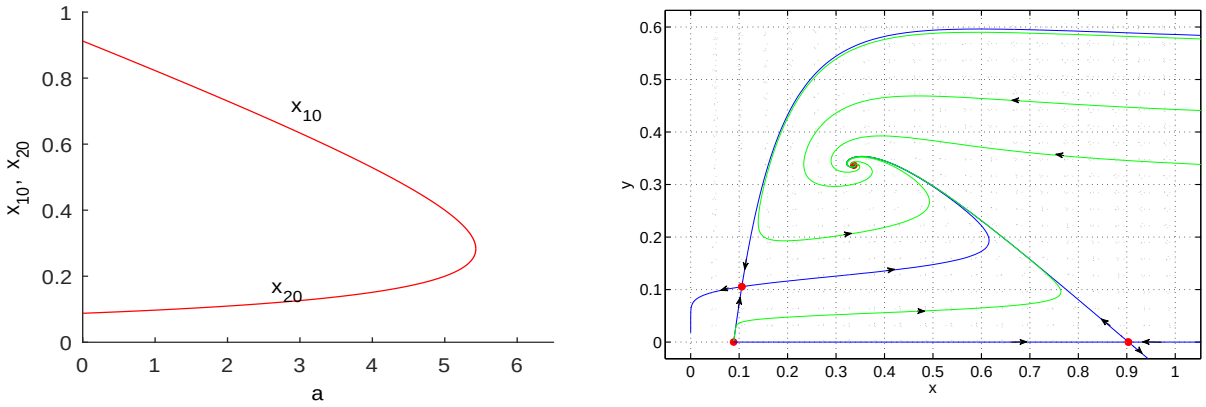

(a) (b)

Figure 1. Fix $(h, b, s) = (0.08, 1.2, 0.1)$. (a) Existence of boundary equilibria of system (1.5) with a as parameter. (b) Phase portrait of system (1.5) with $a = 0.1$.

2.2. *Existence and stability of positive equilibria*

Note that any positive equilibrium of system (1.5) satisfies

$$\begin{aligned} &\frac{x(1-x)}{1+ax} - bxy - h = 0, \\ &1 - \frac{y}{x} = 0. \end{aligned} \tag{2.2}$$

From Eq (2.2), we denote

$$f(x) = abx^3 + (b+1)x^2 + (ah-1)x + h,$$

then

$$f'(x) = 3abx^2 + 2(b+1)x + ah - 1, \tag{2.3}$$

whose discriminant

$$\Delta = 4(b+1)^2 - 12ab(ah-1) > 0, \quad \text{when} \quad ah < 1.$$

Obviously, in the interval $(0, 1)$, $f'(x) = 0$ has a unique positive root

$$x_* = \frac{-2(b+1) + \sqrt{\Delta}}{6ab}.$$

For any positive equilibrium $E(x, y)$, from $f(x) = 0$, we obtain

$$h = -\frac{x(abx^2 + bx + x - 1)}{ax + 1}.$$

Substituting this into $\mathrm{Det}(J_E)$ and $f'(x)$, there is

$$\mathrm{Det}(J_E) = \frac{s}{1+ax} f'(x). \tag{2.4}$$

Theorem 2.2. *For the positive equilibria of system* (1.5)*, the following conclusions hold:*

(1) *If* $ah < 1$ *and* $f(x_*) < 0$*, then system* (1.5) *has two positive equilibria: a hyperbolic saddle* $E_{11}(x_{11}, x_{11})$*, and an elementary and antisaddle equilibrium* $E_{12}(x_{12}, x_{12})$*, with* $x_{11} < x_* < x_{12}$*;*

(2) *if* $ah < 1$ *and* $f(x_*) = 0$*, then system* (1.5) *has a unique positive degenerate equilibrium* $E_*(x_*, x_*)$*;*

(3) *if* $ah \geq 1$ *or* $f(x_*) > 0$*, then system* (1.5) *has no positive equilibrium.*

Proof. From (2.3) and (2.4), it is obvious that $\mathrm{Det}(J_{E_{11}}) < 0$, $\mathrm{Det}(J_{E_{12}}) > 0$ and $\mathrm{Det}(J_{E_*}) = 0$. Thus E_{11} is a hyperbolic saddle, E_{12} is an elementary and antisaddle equilibrium, and E_* is a degenerate equilibrium. The proof is completed.

Next, we consider case (2) of Theorem 2.2. From $f(x_*) = f'(x_*) = 0$, we can express

$$b = b_* = \frac{1 - ax_*^2 - 2x_*}{2x_*(ax_* + 1)^2}, \quad h = h_* = \frac{(1 - ax_*^2 + 2ax_*)x_*}{2(ax_* + 1)^2},$$

furthermore, we let

$$s_* = \frac{1 - ax_*^2 - 2x_*}{2(ax_* + 1)^2}.$$

Theorem 2.3. *Assume that* $b = b_*$*,* $h = h_*$ *and* $a < \frac{1-2x_*}{x_*^2}$ *with* $x_* < \frac{1}{2}$*, then system* (1.5) *admits a degenerate positive equilibrium* $E_*(x_*, x_*)$*. Moreover,*

(1) *If* $s > s_*$ (*or* $0 < s < s_*$)*, then* E_* *is a saddle node, which includes a stable* (*or an unstable*) *parabolic sector in the left;*

(2) *If* $s = s_*$*, then* E_* *is a cusp of codimension* 2*.*

Proof. (1) When $s \neq s_*$, make the following transformation

$$x = x_1 + x_*, \quad y = y_1 + x_*,$$

then system (1.5) can be written as

$$\begin{aligned} \dot{x}_1 &= s_* x_1 - s_* y_1 - \frac{a+1}{(1+ax_*)^3} x_1^2 - b x_1 y_1 + o(|x_1, y_1|^2), \\ \dot{y}_1 &= s x_1 - s y_1 - \frac{s}{x_*} x_1^2 + \frac{2s}{x_*} x_1 y_1 - \frac{s}{x_*} y_1^2 + o(|x_1, y_1|^2). \end{aligned} \tag{2.5}$$

In order to translate the linear part of this system to Jordan form, we make the following transformation:

$$x_1 = -s_*(x_2 - y_2), \quad y_1 = -s_* x_2 + s y_2, \quad \mathrm{d}\tau = (s_* - s)\mathrm{d}t.$$

Then system (2.5) becomes

$$\begin{aligned} \dot{x}_2 &= a_{20} x_2^2 + a_{11} x_2 y_2 + a_{02} y_2^2 + o(|x_2, y_2|^2), \\ \dot{y}_2 &= y_2 + b_{20} x_2^2 + b_{11} x_2 y_1 + b_{02} y_2^2 + o(|x_2, y_2|^2), \end{aligned}$$

where

$$a_{20} = \frac{-sA_1A_2}{A_3}, \quad a_{11} = \frac{-sA_1(2(1+ax_*)^3s + 2(a+1)x_* - A_2)}{A_3},$$
$$a_{02} = \frac{s(4s^2(1+ax_*)^5 + 6s(1+ax_*)^3A_1 + A_1A_2)}{A_3}, \quad b_{20} = \frac{-A_1a_{20}}{2s(1+ax_*)^2},$$
$$b_{11} = \frac{-A_1a_{11}}{2s(1+ax_*)^2}, \quad b_{02} = \frac{4s^3(1+ax_*)^7 + 4s^2(1+ax_*)^5A_1 - (a+1)x_*A_1^2}{(1+ax_*)^2A_3},$$

with

$$\begin{aligned} &A_1 = ax_*^2 + 2x_* - 1, \quad A_2 = a^2x_*^3 + 3ax_*^2 - 3ax_* - 1, \\ &A_3 = x_*(1+ax_*)(2a^2sx_*^2 + ax_*^2 + 4asx_* + 2x_* + 2s - 1)^2. \end{aligned} \tag{2.6}$$

Note that when $a < \frac{1-2x_*}{x_*^2}$ with $x_* < \frac{1}{2}$, $A_1 < 0$, $A_2 < 0$ and $A_3 > 0$, thus $a_{20} < 0$. By Theorem 7.1 in Chapter 2 of Zhang et al. [22], E_* is a saddle node, which includes a stable (or an unstable) parabolic sector in the left if $s > s_*$ (or $0 < s < s_*$).

(2) When $s = s_*$, by the following transformations successively

$$\begin{aligned} &x = x_1 + x_*, \quad y = y_1 + x_*; \\ &x_1 = -s_*x_2, \quad y_1 = -s_*x_2 + y_2, \end{aligned}$$

system (1.5) can be rewritten as

$$\begin{aligned} \dot{x}_2 &= y_2 + \frac{A_1A_2}{4x_*(1+ax_*)^5}x_2^2 + \frac{A_1}{2x_*(1+ax_*)^2}x_2y_2 + o(|x_2, y_2|^2), \\ \dot{y}_2 &= \frac{-A_1^2A_2}{8x_*(1+ax_*)^7}x_2^2 - \frac{A_1^2}{4x_*(1+ax_*)^4}x_2y_2 + \frac{A_1}{2x_*(1+ax_*)^2}y_2^2 + o(|x_2, y_2|^2). \end{aligned} \tag{2.7}$$

By Lemma 3.1 of [18], system (2.7) near the origin is equivalent to

$$\begin{aligned} \dot{X} &= Y + o(|X, Y|^3), \\ \dot{Y} &= DX^2 + \check{E}XY + o(|X, Y|^3), \end{aligned}$$

where

$$D = \frac{-A_1^2A_2}{8x_*(1+ax_*)^7}, \quad \check{E} = \frac{A_1(a^2x_*^3 + 3ax_*^2 - 5ax_* - 2x_* - 1)}{4x_*(1+ax_*)^5}.$$

It is obvious that when $a < \frac{1-2x_*}{x_*^2}$ with $x_* < \frac{1}{2}$, we have $D > 0$ and $\check{E} < 0$, thus E_* is a cusp of codimension 2. The proof is completed.

3. Bifurcations

In this section, we investigate the Bogdanov-Takens bifurcation of codimension 2 and the degenerate Hopf bifurcation of codimension 3.

3.1. Bogdanov-Takens bifurcation of codimension 2

According to Theorem 2.3 (2), system (1.5) may have a Bogdanov-Takens bifurcation of codimension 2 around E_*. Now we choose a and h as bifurcation parameters and obtain the following unfolding

system

$$\begin{aligned} \dot{x} &= \frac{x(1-x)}{1+(a+\lambda_1)x} - b_* xy - (h_* + \lambda_2), \\ \dot{y} &= s_* y\Big(1 - \frac{y}{x}\Big), \end{aligned} \tag{3.1}$$

where $\lambda = (\lambda_1, \lambda_2)$ is a parameter vector in a small neighborhood of $(0, 0)$.

Theorem 3.1. *If the conditions of Theorem* 2.3 (2) *hold, then system* (1.5) *undergoes a Bogdanov–Takens bifurcation of codimension* 2 *around* E_*.

Proof. In order to move E_* to the origin, we make a transformation

$$x = x_1 + x_*, \quad y = y_1 + x_*,$$

then system (3.1) becomes

$$\begin{aligned} \dot{x}_1 &= c_{00} + c_{10}x_1 - s_* y_1 + c_{20}x_1^2 - b_* x_1 y_1 + P_1(x_1, y_1, \lambda), \\ \dot{y}_1 &= s_* x_1 - s_* y_1 - b_* x_1^2 + 2b_* x_1 y_1 - b_* y_1^2 + P_2(x_1, y_1, \lambda), \end{aligned} \tag{3.2}$$

where $P_1(x_1, y_1, \lambda)$ and $P_2(x_1, y_1, \lambda)$ are C^∞ functions of at least third order with respect to (x_1, y_1), and

$$\begin{aligned} c_{00} &= \frac{(x_* - 1)x_*^2\lambda_1}{(1+ax_*)(ax_* + x_*\lambda_1 + 1)} - \lambda_2, \\ c_{10} &= -\frac{(ax_*^2 + 2x_* - 1)(ax_* - x_*\lambda_1 + 1)}{2(ax_* + x_*\lambda_1 + 1)(1+ax_*)^2} + \frac{x_*(x_* - 1)\lambda_1}{(ax_* + x_*\lambda_1 + 1)^2(1+ax_*)}, \\ c_{20} &= -\frac{a + \lambda_1 + 1}{(ax_* + x_*\lambda_1 + 1)^3}. \end{aligned}$$

By the following transformation

$$\begin{aligned} x_2 &= x_1, \\ y_2 &= c_{00} + c_{10}x_1 - s_* y_1 + c_{20}x_1^2 - b_* x_1 y_1 + P_1(x_1, y_1, \lambda), \end{aligned}$$

system (3.2) can be rewritten as

$$\begin{aligned} \dot{x}_2 &= y_2, \\ \dot{y}_2 &= d_{00} + d_{10}x_2 + d_{01}y_2 + d_{20}x_2^2 + d_{11}x_2 y_2 + \frac{2b_*}{s_*}y_2^2 + P_3(x_2, y_2, \lambda), \end{aligned} \tag{3.3}$$

where $P_3(x_2, y_2, \lambda)$ is a C^∞ function of at least third order with respect to (x_2, y_2), and

$$\begin{aligned} d_{00} &= \frac{c_{00}(c_{00}b_* + s_*^2)}{s_*}, \\ d_{10} &= -\frac{c_{00}^2 b_*^2 - 2c_{00}s_*(c_{10} - s_*)b_* - s_*^3(c_{10} - s_*)}{s_*^2}, \\ d_{01} &= -\frac{3c_{00}b_* - c_{10}s_* + s_*^2}{s_*}, \\ d_{20} &= -\frac{c_{00}^2 b_*^3 - 2c_{00}c_{10}b_*^2 s_* + 2c_{00}c_{20}b_* s_*^2 + c_{10}^2 b_* s_*^2 - 2c_{10}b_* s_*^3 + c_{20}s_*^4}{s_*^3}, \\ d_{11} &= -\frac{3c_{00}b_*^2 - 3c_{10}b_* s_* + 2c_{20}s_*^2 + 2b_* s_*^2}{s_*^2}. \end{aligned}$$

Make a transformation

$$x_3 = x_2, \quad y_3 = \Big(1 - \frac{2b_*}{s_*}x_2\Big)y_2, \quad \mathrm{d}t = \Big(1 - \frac{2b_*}{s_*}x_2\Big)\mathrm{d}\tau,$$

still denoting τ as t, then system (3.3) becomes

$$\begin{aligned} &\dot{x}_3 = y_3,\\ &\dot{y}_3 = d_1 + d_2x_3 + d_3y_3 + d_4x_3^2 + d_5x_3y_3 + P_4(x_3, y_3, \lambda), \end{aligned} \tag{3.4}$$

where $P_4(x_3, y_3, \lambda)$ is a C^∞ function of at least third order with respect to (x_3, y_3), and

$$\begin{aligned} &d_1 = d_{00}, \qquad d_2 = d_{10} - \frac{4b_*}{s_*}d_{00}, \qquad d_3 = d_{01},\\ &d_4 = \frac{4b_*^2d_{00} - 4b_*d_{10}s_* + d_{20}s_*^2}{s_*^2}, \qquad d_5 = \frac{d_{11}s_* - 2b_*d_{01}}{s_*}. \end{aligned}$$

Note that when λ_1 and λ_2 are small enough,

$$d_4 = -\frac{A_1A_2}{4x_*(1 + ax_*)^5} < 0,$$

where A_1 and A_2 are given in (2.6).

Let

$$x_4 = x_3, \quad y_4 = \frac{y_3}{\sqrt{-d_4}}, \quad \mathrm{d}\tau = \sqrt{-d_4}\mathrm{d}t,$$

still denoting τ as t, then we can rewrite system (3.4) as

$$\begin{aligned} &\dot{x}_4 = y_4,\\ &\dot{y}_4 = -\frac{d_1}{d_4} - \frac{d_2}{d_4}x_4 + \frac{d_3}{\sqrt{-d_4}}y_4 - x_4^2 + \frac{d_5}{\sqrt{-d_4}}x_4y_4 + P_5(x_4, y_4, \lambda), \end{aligned}$$

where $P_5(x_4, y_4, \lambda)$ is a C^∞ function of at least third order with respect to (x_4, y_4).

It is obvious that when λ_1 and λ_2 are small enough,

$$d_5 = \frac{a^2x_*^3 + 3ax_*^2 - 5ax_* - 2x_* - 1}{2x_*(1 + ax_*)^3} < 0.$$

Making the following transformations successively

$$\begin{aligned} &x_5 = x_4 + \frac{d_2}{2d_4}, \quad y_5 = y_4;\\ &x_6 = \frac{d_5^2}{d_4}x_5, \quad y_6 = \frac{d_5^3}{(-d_4)^{3/2}}y_5, \quad \mathrm{d}\tau = -\frac{\sqrt{-d_4}}{d_5}\mathrm{d}t, \end{aligned}$$

we obtain the following versal unfolding of system (3.1)

$$\begin{aligned} &\dot{x}_6 = y_6,\\ &\dot{y}_6 = \mu_1 + \mu_2y_6 + x_6^2 + x_6y_6 + P_6(x_6, y_6, \lambda), \end{aligned}$$

where $P_6(x_6, y_6, \lambda)$ is a C^∞ function of at least third order with respect to (x_6, y_6), and

$$\mu_1 = \frac{(4d_1d_4 - d_2^2)d_5^4}{4d_4^4}, \qquad \mu_2 = \frac{(2d_3d_4 - d_2d_5)d_5}{2d_4^2}.$$

By Maple software, we can obtain

$$\left|\frac{\partial(\mu_1, \mu_2)}{\partial(\lambda_1, \lambda_2)}\right|_{\lambda=0} = -\frac{2(a^2x_*^3 + 3ax_*^2 - 5ax_* - 2x_* - 1)^5(ax_*^2 + 3x_* - 2)(1 + ax_*)}{(ax_*^2 + 2x_* - 1)^2(a^2x_*^3 + 3ax_*^2 - 3ax_* - 1)^5} > 0.$$

By the results of [23], system (3.1) is the versal unfolding of Bogdanov–Takens sigularity (cusp case) of codimension 2, when $\lambda = (\lambda_1, \lambda_2)$ is a parameter vector in a small neighborhood of $(0, 0)$. Hence, system (1.5) undergoes a Bogdanov-Takens bifurcation of codimension 2. The proof is completed.

3.2. Degenerate Hopf bifurcation of codimension 3

The proof of Theorem 2.2 shows that $\mathrm{Det}(J_{E_{12}}) > 0$, that is, system (1.5) may undergo a Hopf bifurcation around E_{12} when $\mathrm{Tr}(J_{E_{12}}) = 0$. For simplicity, we denote x_{12} by z. From $f(z) = 0$ and $\mathrm{Tr}(J_{E_z}) = 0$, we obtain

$$b = \frac{1 - 2z - az^2 - s(1 + az)^2}{z(1 + az)^2}, \quad h = \frac{z(s(1 + az)^2 + z(a + 1))}{(1 + az)^2}. \tag{3.5}$$

By $b > 0$ and $\mathrm{Det}(J_{E_z}) > 0$, we denote

$$\mathcal{M} := \left\{(a, s, z) \in \mathbb{R}^3_+ \middle| 0 < s < \frac{1 - 2z - az^2}{(1 + az)^2},\ 0 < a < \frac{1 - 2z}{z^2},\ 0 < z < \frac{1}{2}\right\}. \tag{3.6}$$

To obtain the focal values around $E_{12}(z, z + k)$, we make the following transformations successively

$$\begin{aligned}
&\text{(i)} \quad \mathrm{d}t = x(1 + ax)\mathrm{d}\tau_0;\\
&\text{(ii)} \quad x = x_1 + z,\ \ y = y_1 + z;\\
&\text{(iii)} \quad x_1 = x_2 + \frac{\sqrt{D}}{zs(1 + az)}y_2,\ \ y_1 = x_2,\ \ \mathrm{d}\tau = \sqrt{D}\mathrm{d}\tau_0,
\end{aligned}$$

where

$$D = -sz^2(2a^2sz^2 + 4asz + az^2 + 2s + 2z - 1) > 0, \quad \text{for} \quad (a, s, z) \in \mathcal{M}.$$

Still denoting τ by t, system (1.5) can be rewritten as

$$\begin{aligned}
\dot{x}_2 &= y_2 + \bar{a}_{11}x_2y_2 + \bar{a}_{02}y_2^2 + \bar{a}_{21}x_2^2y_2 + \bar{a}_{12}x_2y_2^2,\\
\dot{y}_2 &= -x_2 + \bar{b}_{20}x_2^2 + \bar{b}_{11}x_2y_2 + \bar{b}_{02}y_2^2 + \bar{b}_{30}x_2^3 + \bar{b}_{21}x_2^2y_2 + \bar{b}_{12}x_2y_2^2 + \bar{b}_{03}y_2^3 + \bar{b}_{40}x_2^4\\
&\quad + \bar{b}_{31}x_2^3y_2 + \bar{b}_{22}x_2^2y_2^2 + \bar{b}_{13}x_2y_2^3,
\end{aligned}$$

where

$$\bar{a}_{11} = \frac{2az+1}{z(az+1)}, \quad \bar{a}_{02} = \frac{a\sqrt{D}}{zs(az+1)^2}, \quad \bar{a}_{21} = \frac{a}{z(az+1)}, \quad \bar{a}_{12} = \frac{a\sqrt{D}}{z^2s(az+1)^2},$$
$$\bar{b}_{20} = \frac{szB_1}{(1+az)D}, \quad \bar{b}_{11} = \frac{B_1 - z(a+1)}{(1+az)^2D}, \quad \bar{b}_{02} = \frac{B_1 - B_2 - B_3 - z(a+1)}{sz(az+1)^3},$$
$$\bar{b}_{30} = \frac{sB_2}{(az+1)D}, \quad \bar{b}_{21} = \frac{2B_2 - z(a+1)}{z(az+1)^2\sqrt{D}}, \quad \bar{b}_{12} = \frac{B1 - 2B_3 + az^2 - 2az - 1}{sz^2(az+1)^3},$$
$$\bar{b}_{03} = \frac{(az^2+2z-1-2B_3)(aB_3 - a^2z^2 - 2az - 1)}{(az+1)^4s\sqrt{D}}, \quad \bar{b}_{40} = \frac{asB_3}{(az+1)D},$$
$$\bar{b}_{31} = \frac{3aB_3}{z(az+1)^2\sqrt{D}}, \quad \bar{b}_{22} = \frac{3aB_3}{(az+1)^3sz^2}, \quad \bar{b}_{13} = \frac{aB_3\sqrt{D}}{z^3s^2(az+1)^4},$$
$$B_1 = 5a^3sz^3 + 13a^2sz^2 + 3a^2z^3 + 11asz + 8az^2 - 4az + 3s + 3z - 2,$$
$$B_2 = 4a^3sz^3 + 9a^2sz^2 + 3a^2z^3 + 6asz + 7az^2 - 4az + s + z - 1,$$
$$B_3 = a^2sz^2 + 2asz + az^2 + s + 2z - 1.$$

The first three Lyapunov coefficients [22] at E_{12}, respectively, are

$$L_1 = -\frac{zB_3f_1}{4(az+1)^5D^{3/2}},$$
$$L_2 = -\frac{zB_3f_2}{24s(az+1)^{11}D^{5/2}},$$
$$L_3 = \frac{z^3B_3f_3}{1152s(az+1)^{17}D^{9/2}},$$

where

$$f_1 = (az+1)^6s^2 - z(a+1)(az-5)(az+1)^2s - z(a+1)(2a^2z^3 + 3az^2 - 4az - 4z + 1),$$

and f_2, f_3 are polynomials with respect to a, s and z, whose expressions are omitted.

For the polynomials f, g and h_i $(i = 1, 2, \cdots, n)$, let $V(h_1, h_2, \cdots, h_n)$ be the set of common zeros of h_i $(i = 1, 2, \cdots, n)$, $\mathrm{res}(f, g, x)$ be the Sylvester resultant of f and g with respect to x, and $\mathrm{lcoeff}(f, x)$ be the leading coefficient of f with respect to x. By Maple software, we can obtain

$$r_{12} = \mathrm{res}(f_1, f_2, s) = z^3(a+1)^3(az+1)^{22}P_1P_2P_3g_1,$$
$$r_{13} = \mathrm{res}(f_l, f_3, s) = -4z^4(a+1)^4(az+1)^{39}P_1P_2P_3g_2,$$
$$r_{23} = \mathrm{res}(f_2, f_3, s) = -3z^{12}(a+1)^9(az^2+2z-1)^3(az+1)^{92}P_1P_2P_3g_3,$$
$$\bar{r}_{12} = \mathrm{res}(g_1, g_2, a) = c_1z^{391}(2z-5)(25z^2+20z-94)(z-1)^{107}P_4h_1h_2,$$
$$\bar{r}_{13} = \mathrm{res}(g_1, g_3, a) = c_2z^{995}(2z-5)(z-1)^{267}P_4h_1h_3,$$

where

$$P_1 = a^2z^3 + 3az^2 - 3az - 1, \qquad P_2 = 2a^2z^3 + 3az^2 - 4az - 4z + 1,$$
$$P_3 = a^2z^3 + 3az^2 - 5az - 2z - 1, \quad P_4 = 113z^3 - 153z^2 + 46z - 22,$$
$$c_1 = 3259867590634045802246936985600,$$
$$c_2 = 8156188036920358484088762557661080853676032000000,$$

g_i $(1 = 1, 2, 3)$ are polynomials with respect to a and z, h_i $(1 = 1, 2, 3)$ are polynomials with respect to z, and their expressions are omitted.

Let

$$l_1 = \text{lcoeff}(f_1, s) = (az + 1)^6 > 0,$$
$$l_2 = \text{lcoeff}(f_2, s) = 3(3az + 5)(4az + 3)(az + 1)^{12} > 0,$$
$$l_3 = \text{lcoeff}(g_1, a) = 8z^{16} > 0.$$

Theorem 3.2. *Assume that* (3.5) *and* (3.6) *hold, then E_z is a weak focus of order at most* 3.

Proof. Note that $B_3 < 0$ in $\mathcal{M}$, thus

$$V(L_1, L_2, L_3) \cap \mathcal{M} = V(f_1, f_2, f_3) \cap \mathcal{M}.$$

We can easily verify that $P_1 < 0$, $P_3 < 0$, $P_4 < 0$ and $25z^2 + 20z - 94 < 0$ in $\mathcal{M}$. Then by Lemma 2 in Chen and Zhang [24], we obtain the following decomposition

$$V(f_1, f_2, f_3) \cap \mathcal{M} = (V_1 \cup V_2 \cup V_3) \cap \mathcal{M},$$

where

$$V_1 = V(f_1, f_2, f_3, P_2), \quad V_2 = V(f_1, f_2, f_3, g_1, g_2, g_3, h_1), \quad V_3 = V(f_1, f_2, f_3, g_1, g_2, g_3, h_2, h_3).$$

Next, we prove $V(L_1, L_2, L_3) \cap \mathcal{M} = \emptyset$ by three steps.

Step 1. Proving that $V_1 \cap \mathcal{M} = \emptyset$. We can easily verify that $P_2 < 0$ when $\frac{1}{4} \le z < \frac{1}{2}$, and when $0 < z < \frac{1}{4}$, in $\mathcal{M}$, $P_2 = 0$ has a unique positive root

$$a_1 = \frac{4 - 3z - \sqrt{41z^2 - 32z + 16}}{4z^2}.$$

Note that $5 - a_1 z > 0$ when $0 < z < \frac{1}{4}$, which leads to

$$f_1 = (az + 1)^6 s^2 - z(a + 1)(az - 5)(az + 1)^2 s - z(a + 1)P_2 > 0, \quad \text{for} \quad a = a_1.$$

Thus, $V_1 \cap \mathcal{M} = \emptyset$.

Step 2. Proving that $V_2 \cap \mathcal{M} = \emptyset$. Note that

$$V_2 = V(f_1, g_1, h_1) \cap V(f_2, f_3, g_2, g_3).$$

By the command "realroot($h_1, 10^{-30}$)", $h_1(z)$ exists only one positive real root isolation interval $[\underline{z}, \overline{z}] \subset (0, \frac{1}{2})$, where

$$\underline{z} = \frac{5361020705546667481540567750401}{40564819207303340847894502572032},$$
$$\overline{z} = \frac{26805103527733337407702838752 01}{20282409603651670423947251286016}.$$

For the real root interval $[\underline{z}, \overline{z}]$ of $h_1(z)$, using the real root isolation algorithm of multivariate polynomial systems [25], we can obtain a unique positive real root isolation interval $[\underline{a}, \overline{a}]$ in $\mathcal{M}$, where

$$\underline{a} = \frac{120105761319427006491034363832 33}{10141204801825835211973625643008},$$
$$\overline{a} = \frac{60052880659713503245517181916 19}{50706024009129176059868128215 04}.$$

Note that

$$az - 5 \le \bar{a}\bar{z} - 5 < 0,$$
$$2a^2z^3 + 3az^2 - 4az - 4z + 1 \le 2\bar{a}^2\bar{z}^3 + 3\bar{a}\bar{z}^2 - 4\underline{a}\,\underline{z} - 4\underline{z} + 1 < 0.$$

This means $f_1(s, a, z) > 0$ in the real root isolation interval $[\underline{z}, \overline{z}] \times [\underline{a}, \overline{a}]$ of $\{h_1, g_1\}$. Thus $V_2 \subseteq V(f_1, g_1, h_1) = \emptyset$, which implies $V_2 \cap \mathcal{M} = \emptyset$.

Step 3. Proving that $V_3 \cap \mathcal{M} = \emptyset$**.** By Maple software, there is

$$\mathrm{res}(h_2, h_3, z) < 0,$$

which implies $V(h_2, h_3) = \emptyset$. Therefore, $V_3 \cap \mathcal{M} = \emptyset$.

To sum up, we show that $V(f_1, f_2, f_3) \cap \mathcal{M} = \emptyset$. Thus E_z is a weak focus of order at most 3. The proof is completed.

Define

$$\begin{aligned}
\mathcal{M}_1 &:= \{(a, s, z) \in \mathcal{M} : f_1(a, s, z) \neq 0\},\\
\mathcal{M}_2 &:= \{(a, s, z) \in \mathcal{M} : f_1(a, s, z) = 0,\ f_2(a, s, z) \neq 0\},\\
\mathcal{M}_3 &:= \{(a, s, z) \in \mathcal{M} : f_1(a, s, z) = 0,\ f_2(a, s, z) = 0\}.
\end{aligned}$$

From Theorem 3.2, we have the following theorem.

Theorem 3.3. *Assume that* (3.5) *and* (3.6) *hold, then E_z is a weak focus of order up to* 3*. Moreover,*
(1) *if $(a, s, z) \in \mathcal{M}_1$, then E_z is a weak focus of order* 1*;*
(2) *if $(a, s, z) \in \mathcal{M}_2$, then E_z is a weak focus of order* 2*;*
(3) *if $(a, s, z) \in \mathcal{M}_3$, then E_z is a weak focus of order* 3*.*

To verify $\mathcal{M}_3 \neq \emptyset$, we let $z = \frac{1}{20}$. Again from $f(z) = 0$ and $\mathrm{Tr}(J_{E_z}) = 0$, we have

$$b = \bar{b} := -\frac{20(a^2s + 40as + a + 400s - 360)}{(a + 20)^2}, \quad h = \bar{h} := \frac{a^2s + 40as + 20a + 400s + 20}{20(a + 20)^2}. \tag{3.7}$$

By $b > 0,\ h > 0$ and $\mathrm{Det}(J_{E_z}) > 0$, we define

$$\mathcal{M}_* := \left\{(a, s) \in \mathbb{R}^2_+ \middle| 0 < s < \frac{360 - a}{(a + 20)^2},\ 0 < a < 360\right\}. \tag{3.8}$$

We can obtain the following theorem.

Theorem 3.4. *When $z = \frac{1}{20}$, assume that* (3.7) *and* (3.8) *hold, and there exist $a_0 \in [\underline{a}_0, \overline{a}_0]$ and $s_0 \in [\underline{s}, \overline{s}]$ given respectively in* (3.9) *and* (3.10)*, then E_z is a weak focus of order* 3 *and system* (1.5) *can undergo a degenerate Hopf bifurcation of codimension* 3 *near E_z.*

Proof. When $z = \frac{1}{20}$, by the command "realroot($g_1, 10^{-30}$)", $g_1(a, \frac{1}{2})$ exists a positive real root isolation interval $[\underline{a}_0, \overline{a}_0]$ in $\mathcal{M}_*$, where

$$\begin{aligned}
\underline{a}_0 &= \frac{5874835427557719832996668109293}{40564819207303340847894502572032},\\
\overline{a}_0 &= \frac{2937417713778859916498334054647}{20282409603651670423947251286016}.
\end{aligned} \tag{3.9}$$

For the real root interval $[\underline{a}_0, \overline{a}_0]$ of $g_1(a, \frac{1}{2})$, using the real root isolation algorithm of multivariate polynomial systems [25], we can obtain a unique positive real root isolation interval $[\underline{s}, \overline{s}]$ in $\mathcal{M}_*$, where

$$\begin{aligned} \underline{s} &= \frac{16366657194970570012540109517554067432784854345 1435}{14965776766268445882405732687014738121276749240074 24}, \\ \overline{s} &= \frac{65466628779882280050160438070218030308439223238 6479}{59863107065073783529622930748058952485106996960296 96}. \end{aligned} \tag{3.10}$$

Hence, under the conditions (3.7) and (3.8), when $z = \frac{1}{20}$, there exist $a_0 \in [\underline{a}_0, \overline{a}_0]$ and $s_0 \in [\underline{s}, \overline{s}]$ such that $f_1(a_0, s_0, \frac{1}{20}) = f_2(a_0, s_0, \frac{1}{20}) = 0$. Therefore, according to Theorem 3.2, E_z is a weak focus of order exactly 3.

Finally,

$$\left|\frac{\partial(\mathrm{Tr}(J_{E_z}), L_1, L_2)}{\partial(a, s, z)}\right|_{z=\frac{1}{20}} = -\frac{100000(a^2 s + 40as + a + 400s - 360)J(a, s)}{3(a + 20)^{19} s^6 (2a^2 s + 80as + a + 800s - 360)^5},$$

where the expression of $J(a, s)$ is too long and is omitted here.

For the polynomial $f(x, y)$, let $f^+(x, y)$ and $f^-(x, y)$ be the summations of the positive and negative terms in $f(x, y)$, respectively ([25]).

According to Theorem 2.2 in [25], we have

$$J(a, s) < J^+(\overline{a}_0, \overline{s}) + J^-(\underline{a}_0, \underline{s}) \approx -1.739971526 \times 10^{32} < 0.$$

Note that $a^2 s + 40as + a + 400s - 360 \neq 0$, thus $\left|\frac{\partial(\mathrm{Tr}(J_{E_z}), L_1, L_2)}{\partial(a, s, z)}\right| \neq 0$, for $(a, s, z) = (a_0, s_0, \frac{1}{20})$. Therefore, system (1.5) can undergo a degenerate Hopf bifurcation of codimension 3 near E_z. The proof is completed.

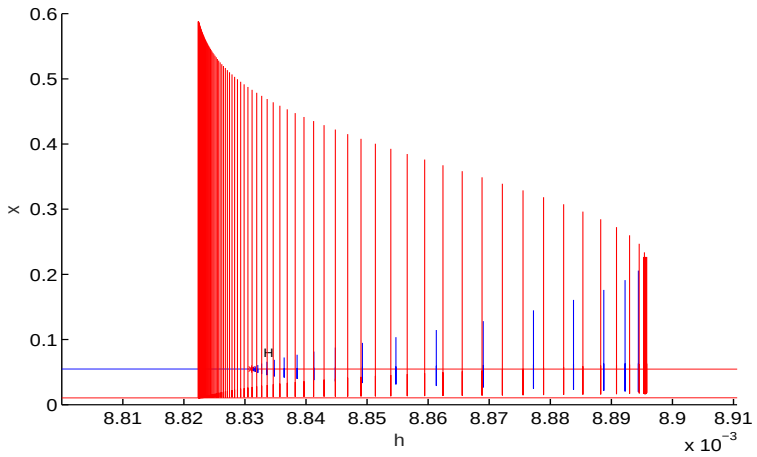

Figure 2. Bifurcation diagram of system (1.5) in (h, x)-plane with $(a, b, s) = (0.142, 14.2, 0.1)$, where the blue and red lines respectively represent stable and unstable limit cycles or equilibria.

4. Numerical simulations

In this section, we give some numerical simulations by Matcont to support the bifurcation phenomena of system (1.5).

Choose $a = 0.142$, $b = 14.2$, and $s = 0.1$, and present the bifurcation diagram in the (h, x)-plane by Matcont. Figure 2 shows that when $0 < h < 0.0088222644$, the positive equilibrium E_{12} is stable and system (1.5) has no limit cycle; when $0.0088222644 < h < 0.0088313334$, system (1.5) admits an unstable limit cycle around E_{12}; when $0.0088313334 < h < 0.0088955378$, system (1.5) has two limit cycles, where the inner one is stable and the outer one is unstable; and when $h > 0.0088955378$, the positive equilibrium E_{12} is unstable and system (1.5) has no limit cycle. It is shown that when the constant-yield prey harvesting h is relatively small, the constant-yield prey harvesting does not change the dynamic behaviors of the system, that is, both populations will coexist in fixed sizes E_{12}; as h increases, system (1.5) first generates an unstable limit cycle and then two limit cycles (the inner one is stable); but when h is relatively large, the limit cycles will disappear first and then the positive equilibria, and finally there will be no positive equilibrium point.

In Figure 3, we present the corresponding phase portraits of system (1.5) with $a = 0.142$, $b = 14.2$, and $s = 0.1$, as h varies. When $h = 0.008$, from Figure 3(a), the positive equilibrium E_{12} is stable, that is, when the initial values (i.e. initial densities of both populations) lie inside the region to the right of the stable manifold of the saddle E_{11}, both populations will coexist in fixed sizes E_{12}; when $h = 0.00883$, from Figure 3(b), system (1.5) admits a unstable limit cycle, that is, when the initial values lie inside the unstable limit cycle, both populations will coexist in fixed sizes E_{12}; when $h = 0.00888$, from Figure 3(c), system (1.5) admits two limit cycles (the inner one is stable), that is, when the initial values lie inside the outer limit cycle, both populations will coexist in the stable limit cycle; otherwise, both populations will not coexist in the above three figures. When $h = 0.0098$, from Figure 3(d), all the nonnegative equilibria are unstable, that is, both populations will not coexist. Hence the relatively small harvesting can make both populations coexist in fixed sizes or in a periodic orbit; that is, the small harvesting can affect the populations of both species to some extent; however, the large harvesting is detrimental to the dynamic behaviors of the system.

5. Conclusions

In this paper, we discussed the stability and bifurcation of a Leslie–Gower predator–prey model with Smith growth and constant-yield harvesting. We proved that system (1.5) admits at most two boundary equilibria, both of which are unstable. For system (1.5) without Smith growth, that is system (1.3), Zhu and Lan [21] investigated the stability of equilibria. Also, system (1.3) undergoes the saddle-node bifurcation and supercritical and subcritical Hopf bifurcations. Compared with the results in [21], we presented some different dynamics of the system, and found that both the Smith growth and constant-yield harvesting play important roles in the dynamics of system (1.5), more precisely, we proved that the degenerate positive equilibrium of system (1.5) is a cusp of codimension 2 and system (1.5) undergoes cusp-type Bogdanov–Takens bifurcation of codimension 2. Further, using the resultant elimination method and the real root isolation algorithm of multivariate polynomial systems [25], we proved that system (1.5) has a weak focus of order at most 3 and undergoes a degenerate Hopf bifurcation of codimension 3. By numerical simulation, we illustrated that system (1.5) has

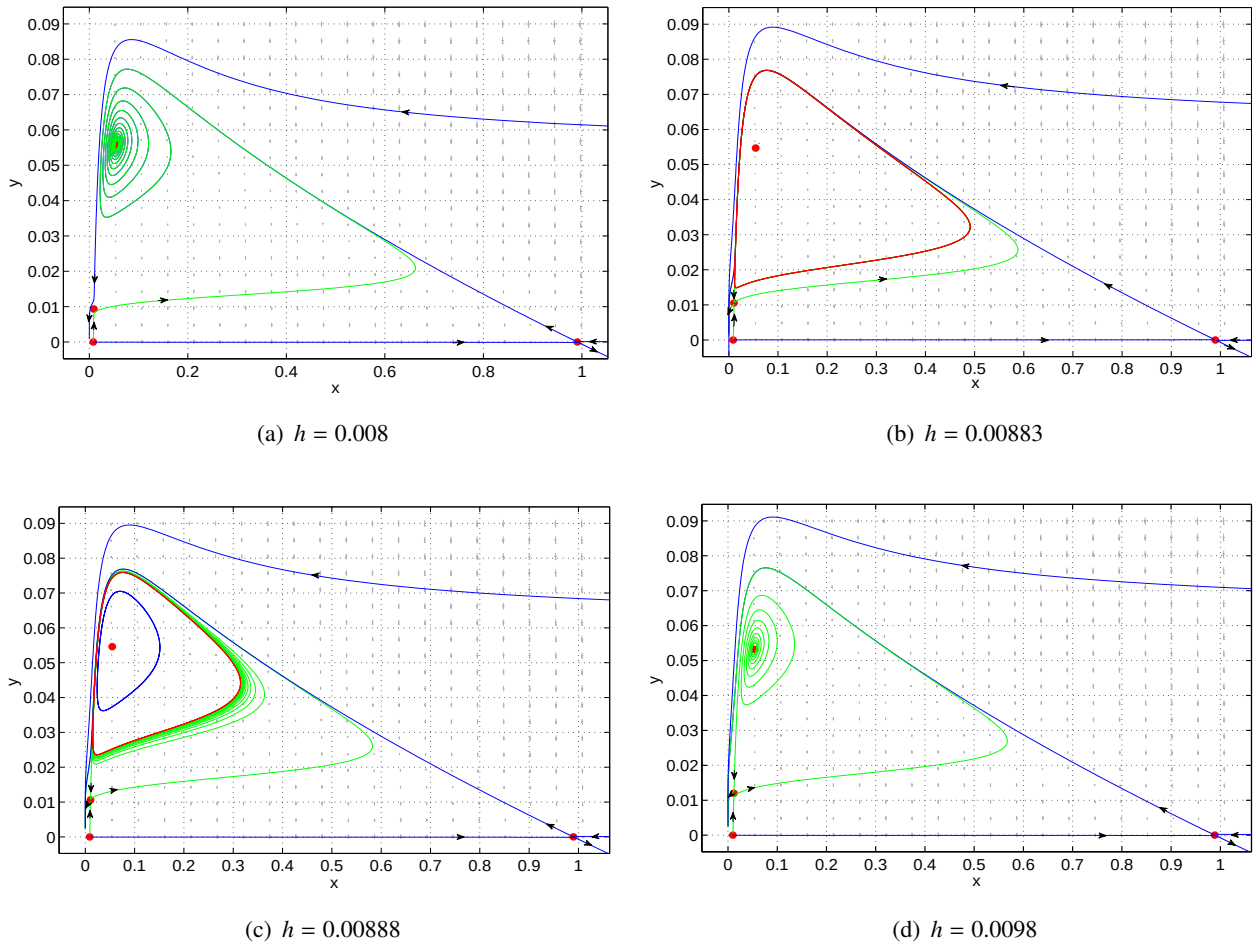

(a) $h = 0.008$

(b) $h = 0.00883$

(c) $h = 0.00888$

(d) $h = 0.0098$

Figure 3. Phase portraits of system (1.5) with $(a, b, s) = (0.142, 14.2, 0.1)$, where the blue and red cycles respectively represent stable and unstable limit cycles.

two limit cycles (the inner one is stable). Also, we showed that the small harvesting is conducive to the survival of prey and predators, but the large harvesting is detrimental to the coexistence of the populations. Therefore, our results revealed that Smith growth and constant-yield harvesting can lead to richer dynamic behaviors.

Motivated by Lampart and Zapomĕl [26], whether there are some new numerical methods to derive some new dynamical behaviors. Also, we can regard the presence of more complex phenomena such as intermittency (see [27]) of the system in the future.

Use of AI tools declaration

The authors declare they have not used Artificial Intelligence (AI) tools in the creation of this article.

Acknowledgements

This work was supported by the Natural Science Foundation of Fujian Province (2021J01613, 2021J011032, 2023J05250) and the Scientific Research Foundation of Minjiang University (MJY22027).

Conflict of interest

The authors declare there is no conflict of interest.

References

1. P. H. Leslie, Some further notes on the use of matrices in population mathematics, *Biometrika*, **35** (1948), 213–245. https://doi.org/10.2307/2332342
2. P. H. Leslie, A stochastic model for studying the properties of certain biological systems by numerical methods, *Biometrika*, **45** (1958),16–31. https://doi.org/10.2307/2333042
3. A. Korobeinikov, A Lyapunov function for Leslie–Gower predator–prey models, *Appl. Math. Lett.*, **14** (2001), 697–699. https://doi.org/10.1016/s0893-9659(01)80029-x
4. S. B. Hsu, T. W. Huang, Global stability for a class of predator–prey system, *SIAM J. Appl. Math.*, **55** (1995), 763–783. https://doi.org/10.1137/s0036139993253201
5. J. C. Huang, S. G. Ruan, J. Song, Bifurcations in a predator–prey system of Leslie type with generalized Holling type III functional response, *J. Differ. Equations*, **257** (2014), 1721–1752. https://doi.org/10.1016/j.jde.2014.04.024
6. Y. F. Dai, Y. L. Zhao, B. Sang, Four limit cycles in a predator–prey system of Leslie type with generalized Holling type III functional response, *Nonlinear Anal. Real World Appl.*, **50** (2019), 218–239. https://doi.org/10.1016/j.nonrwa.2019.04.003
7. M. X. He, Z. Li, Global dynamics of a Leslie-Gower predator-prey model with square root response function, *Appl. Math. Lett.*, **140** (2023), 108561. https://doi.org/10.1016/j.aml.2022.108561
8. Y. F. Wu, X. H. Ai, Analysis of a stochastic Leslie-Gower predator–prey system with Beddington-DeAngelis and Ornstein-Uhlenbeck process, *Electron. Res. Arch.*, **32** (2024), 370-385. https://doi.org/10.3934/era.2024018
9. J. Xu, Y. Tian, H. J. Guo, X. Y. Song, Dynamical analysis of a pest management Leslie-Gower model with ratio-dependent functional response, *Nonlinear Dyn.*, **93** (2018), 507-720. https://doi.10.1007/s11071-018-4219-9
10. Y. Tian, X. R. Yan, K. B. Sun, Dual effects of additional food supply and threshold control on the dynamics of a Leslie-Gower model with pest herd behavior, *Chaos Solitons Fractals*, **185** (2024), 115163. https://doi.org/10.1016/j.chaos.2024.115163
11. F. E. Smith, Population dynamics in Daphnia magna and a new model for population growth, *Ecology*, **44** (1963), 651–663. https://doi.org/10.2307/1933011

12. V. Kumar, Pattern formation and delay-induced instability in a Leslie-Gower type prey–predator system with Smith growth function, *Math. Comput. Simulat.*, **225** (2024), 78–97. https://doi.org/10.1016/j.matcom.2024.05.004

13. Z. Li, M. X. He, Hopf bifurcation in a delayed food-limited model with feedback control, *Nonlinear Dyn.*, **76** (2014), 1215–1224. https://doi.org/10.1007/s11071-013-1205-0

14. X. Z. Feng, X. Liu, C. Sun, Y. L. Jiang, Stability and Hopf bifurcation of a modified Leslie-Gower predator–prey model with Smith growth rate and B-D functional response, *Chaos Solitons Fractals*, **174** (2023), 113794. https://doi.org/10.1016/j.chaos.2023.113794

15. D. Bai, J. Zheng, Y. Kang, Global dynamics of a predator-prey model with a Smith growth function and the additive predation in prey, *Discrete Continuous Dyn. Syst. Ser. B*, **29** (2024), 1923–1960. https://doi.org/10.3934/dcdsb.2023161

16. X. L. Han, C. Y. Lei, Bifurcation and turing instability analysis for a space- and time-discrete predator-prey system with Smith growth function, *Chaos Solitons Fractals*, **166** (2023), 112910. https://doi.org/10.1016/j.chaos.2022.112910

17. H. Guo, Y. Tian, K. B. Sun, X. Y. Song, Dynamic analysis of two fishery capture models with a variable search rate and fuzzy biological parameters, *Math. Biosci. Eng.*, **20** (2023), 21049–21074. https://doi.org/10.3934/mbe.2023931

18. J. C. Huang, Y. J. Gong, S. G. Ruan, Bifurcations analysis in a predator-prey model with constant-yield predator harvesting, *Discrete Continuous Dyn. Syst. Ser. B*, **18** (2013), 2101–2121. https://doi.org/10.3934/dcdsb.2013.18.2101

19. Y. C. Xu, Y. Yang, F. W. Meng, S. G. Ruan, Degenerate codimension-2 cusp of limit cycles in a Holling-Tanner model with harvesting and anti-predator behavior, *Nonlinear Anal. Real World Appl.*, **76** (2024), 103995. https://doi.org/10.1016/j.nonrwa.2023.103995

20. H. Wu, Z. Li, M. X. He, Bifurcation analysis of a Holling-Tanner model with generalist predator and constant-yield harvesting, *Int. J. Bifurcation Chaos*, **34** (2024), 2450076. https://doi.org/10.1142/s0218127424500767

21. C. R. Zhu, K. Q. Lan, Phase portraits, Hopf bifurcations and limit cycles of Leslie–Gower predator-prey systems with harvesting rates, *Discrete Continuous Dyn. Syst. Ser. B*, **14** (2010), 289–306. https://doi.org/10.3934/dcdsb.2010.14.289

22. Z. F. Zhang, T. R. Ding, W. Z. Huang, Z. X. Dong, *Qualitative Theory of Differential Equations*, Translations of Mathematical Monographs, American Mathematical Society, 1992. https://doi.org/10.1090/mmono/101

23. L. Perko, *Differential Equations and Dynamical Systems*, Springer, New York, 1996. https://doi.org/10.1007/978-1-4684-0392-3

24. X. W. Chen, W. N. Zhang, Decomposition of algebraic sets and applications to weak centers of cubic systems, *J. Comput. Appl. Math.*, **23** (2009), 565–581. https://doi.org/10.1016/j.cam.2009.06.029

25. Z. Lu, B. He, Y. Lou, L. Pan, An algorithm of real root isolation for polynomial systems with application to the construction of limit cycles, *Symb. Numer. Comput.*, **232** (2007), 131–147. https://doi.org/10.1007/978-3-7643-7984-1_9

26. M. Lampart, J. Zapoměl, The disturbance influence on vibration of a belt device driven by a crank mechanism, *Chaos Solitons Fractals*, **173** (2023), 113634. https://doi.org/10.1016/j.chaos.2023.113634

27. A. Lampartová, M. Lampart, Exploring diverse trajectory patterns in nonlinear dynamic systems, *Chaos Solitons Fractals*, **182** (2024), 114863. https://doi.org/10.1016/j.chaos.2024.114863

AIMS Press